

Autoclaving as a chemical-free process to stabilize recombinant silk-elastinlike protein polymer nanofibers

Weiguo Qiu,¹ Joseph Cappello,¹ and Xiaoyi Wu^{1,2,a)}

¹Department of Aerospace and Mechanical Engineering, University of Arizona, Tucson, Arizona 85721, USA

²Biomedical Engineering IDP and Bio5 Institute, University of Arizona, Tucson, Arizona 85721, USA

(Received 4 March 2011; accepted 30 May 2011; published online 28 June 2011)

We report here that autoclaving is a chemical-free, physical crosslinking strategy capable of stabilizing electrospun recombinant silk-elastinlike protein (SELP) polymer nanofibers. Fourier transform infrared spectroscopy showed that the autoclaving of SELP nanofibers induced a conformational conversion of β -turns and unordered structures to ordered β -sheets. Tensile stress-strain analysis of the autoclaved SELP nanofibrous scaffolds in phosphate buffered saline at 37 °C revealed a Young's modulus of 1.02 ± 0.28 MPa, an ultimate tensile strength of 0.34 ± 0.04 MPa, and a strain at failure of $29\% \pm 3\%$. © 2011 American Institute of Physics.

[doi:10.1063/1.3604786]

Because of their outstanding mechanical and biocompatible properties, silk proteins from the silkworm silk have been widely used as biomaterials for use as medical sutures, drug delivery, and tissue engineering materials.¹ The advent of recombinant deoxyribonucleic acid technology has enabled the introduction of structural and/or functional polypeptide sequences into silk-based materials, providing useful properties not obtainable from the native silk proteins alone.² In particular, a series of silk-elastinlike proteins (SELPs) consisting of polypeptide sequences derived from silkworm silk and mammalian elastin have been produced.³ The elastinlike blocks decrease the degree of crosslinking of the silklike blocks, rendering SELPs water soluble,⁴ although native silks are not soluble in either water, dilute acid, or alkali.¹ Consequently, a variety of useful structures, including hydrogels,⁴ films,⁵ and fibers,⁶ have been prepared from SELP in aqueous solution. However, cytotoxic chemicals such as methanol and glutaraldehyde are often used to improve the mechanical strength of the materials for tissue engineering applications by enhancing the bonding of the silklike blocks and/or chemically crosslinking of the SELP micro/nanofibers.^{7,8} Here, we report a chemical-free method to stabilize SELP fibrous structures using autoclaving.

The SELP-47K protein polymer was electrospun into nanofibers as previously reported⁷ and detailed in a supplementary material.⁹ The generated SELP-47K nanofibers, which were collected on aluminum foil, were analyzed using a Hitach-4800s field emission scanning electron microscope (SEM). The SEM analysis revealed that the resulting SELP nanofibers possessed an average diameter of 182 nm [Fig. 1(a)]. Electrospun SELP-47K nanofibers along with the fiber collector were autoclaved at 134 °C and 29 psi for 60 min (Tuttnauer 2340M autoclaver) and vacuum dried overnight prior to SEM analysis. The obtained SEM images were analyzed using the National Institutes of Health (NIH) developed IMAGEJ software to determine the Feret's diameters of the nanofibers and the Feret's pore sizes of the nanofibrous

scaffolds. The thickness of the nanofibrous scaffolds were measured using optical microscopy.⁷ Compared to as-spun scaffolds, autoclaved SELP-47K nanofibrous scaffolds displayed comparable fiber diameters (182 ± 105 nm versus 180 ± 105 nm, $n = 194$) but a slight reduction in pore size (1.07 ± 0.42 μm versus 1.28 ± 0.54 μm , $n = 137$) [Fig. 1(b)]. A pronounced decrease in scaffold thickness, from 200 ± 5 μm to 57 ± 5 μm ($n = 5$), was also observed after autoclaving. When fully rehydrated in $1\times$ phosphate buffered saline

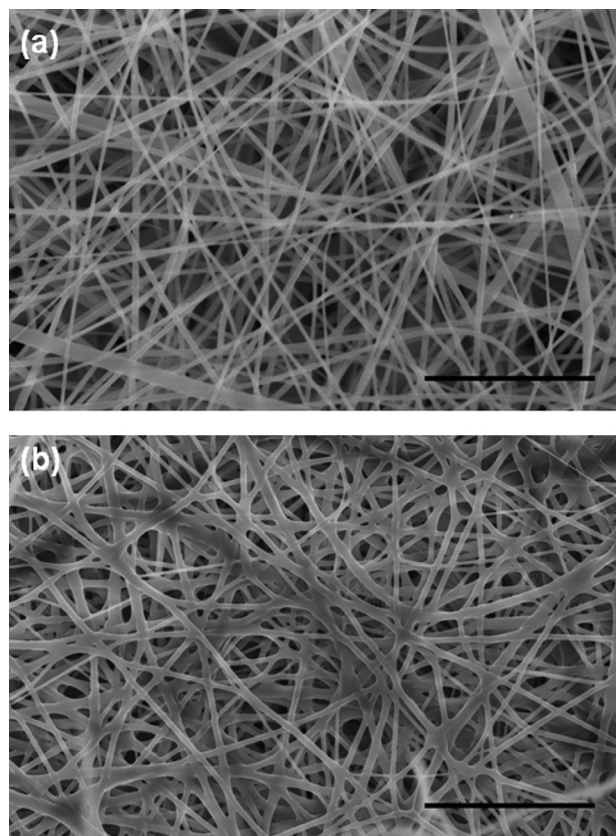


FIG. 1. SEM images of as-spun (a) and autoclaved SELP-47K nanofibers (b). Scale bars: 5 μm .

^{a)}Electronic mail: xwu@email.arizona.edu.

(PBS) at 37 °C, the autoclaved nanofibrous scaffolds were $118.2 \pm 21.5 \mu\text{m}$ ($n = 5$) thick, exhibiting a partial recovery in thickness. Because the scaffolds remained attached to the collector during the autoclaving process, reduction in their lateral dimensions was prevented. Accordingly, rehydration did not lead to any changes in the width and length of autoclaved nanofibrous scaffolds. In marked contrast to the water-soluble as-spun nanofibers, the autoclaved SELP-47K nanofibers were morphologically stable in water. Moreover, the autoclaved nanofibers displayed inter-fiber bonding [Fig. 1(b)].

To understand the autoclaving-induced changes in fiber secondary structure and the subsequent improvement in fiber stability, SELP-47K nanofibers that were autoclaved for specific times (i.e., 15, 30, and 60 min) were analyzed using Fourier transform infrared (FTIR) spectroscopy. The FTIR spectra of as-spun and autoclaved nanofibers were collected using a Magna-IR 560 Nicolet spectrometer (Madison, WI) with CO₂-free dry air as the purging gas.⁹ For each type of nanofiber, 400 scans were collected on triplicate specimens in the spectral range of 4000-800 cm⁻¹ at the resolution of 4 cm⁻¹. The secondary structures of SELP-47K nanofibers were determined by curve fitting of the Fourier self-deconvolved (FSD) amide I bands with Gaussian band profiles [Fig. 2]. The secondary-derivative method was used to identify individual characteristic bands of the FSD amide I bands.¹⁰ Areas under individual bands normalized by the total area of the amide I band represent the percentage contents of secondary structures of the nanofibers.⁹ Specifically, the band at 1616 cm⁻¹ was assigned to aggregated strands, while bands at 1624, 1635, 1675, and 1695 cm⁻¹ were assigned to β -sheet and sheetlike structure.¹⁰ Bands at 1662, 1669, and 1684 cm⁻¹ were assigned to β -turns. Bands at 1646 and 1653 cm⁻¹ were assigned to unordered structures and α -helix, respectively.

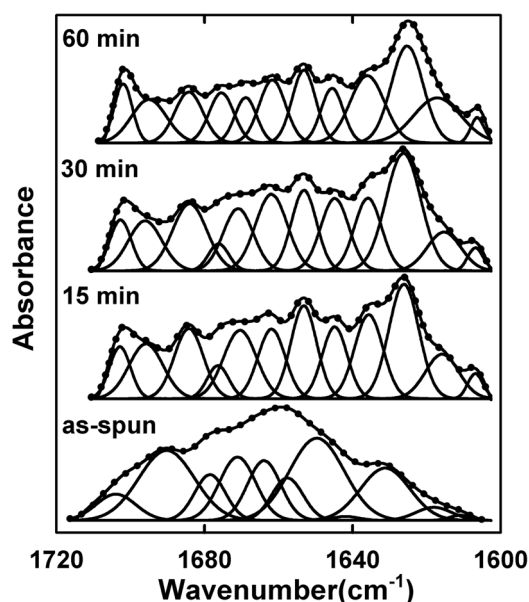


FIG. 2. The FSD FTIR amide I spectra of SELP-47K as-spun nanofibers and nanofibers autoclaved for specific times (i.e., 15, 30, and 60 min) were fitted with Gaussian band profiles. The solid line and dots represent the FSD amide I spectra and the fitted curves, respectively.

TABLE I. Percentages of secondary structure as determined by curve fitting the FSD amide I bands of SELP-47K nanofibers.

	Aggregated strands	β -sheet	β -turn	Unordered structure	α -helix
As-spun	3	31	37	23	7
Autoclaved for 15 min	9	43	29	8	11
Autoclaved for 30 min	8	44	30	9	9
Autoclaved for 60 min	13	50	21	7	9

The quantitative analysis of the FSD amide I spectra of the as-spun SELP-47K nanofibers revealed 37.0% β -turns and 22.8% unordered structures (Table I). When autoclaved for 15 min, the β -turns and unordered structures in SELP-47K nanofibers decreased from 37% to 28.4% and from 22.8% to 8.3%, respectively. Consequently, β -sheets and sheet-like structures increased from 30.5% to 43.6%. Aggregated strands, which were more extensively hydrogen-bonded, increased from 3.0% to 8.6%. FTIR analysis thus produced an autoclaving-induced conformational conversion of less ordered structures (e.g., β -turns, unordered structures) to ordered β -sheets and aggregated strands in SELP-47K nanofibers. Increasing the autoclaving time from 30 to 60 min only slightly enhanced this conversion.

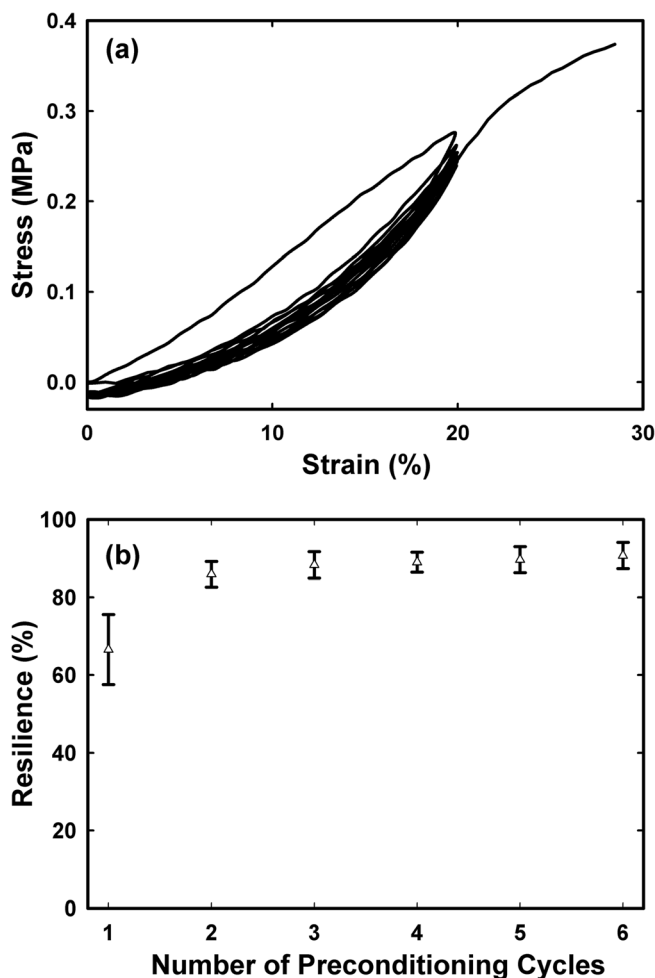


FIG. 3. (a) Representative mechanical preconditioning behavior of autoclaved SELP-47K nanofibrous scaffolds. (b) Resilience of autoclaved SELP-47K nanofibrous scaffold as a function of the number of preconditioning cycles. Data and error bars represent measurements conducted on five replicate samples.

Silk-based materials often exist in two distinct forms: silk I comprised of less ordered conformations (e.g., β -turns, unordered structures) and silk II largely consisting of ordered β -sheets.¹¹ The conversion of silk I to silk II in insects via concurrent shear deformation and water removal establishes the basis for the superior mechanical properties of silk fibers.¹² Nevertheless, it remains a daunting challenge to recapitulate this natural fiber forming process for engineering robust silk-based micro/nanofibers.¹³ Instead, silk-based materials are often stabilized by exposure to cytotoxic, non-solvents such as methanol.¹² Previously, we reported that methanol treatment indeed induced the conversion of silk I to silk II in SELP-47K films⁵ and nanofibers,⁷ leading to the formation of mechanically robust structures. Here, we demonstrate that autoclaving of SELP-47K nanofibers can induce the same conformational conversion, providing a green process for producing stable fibers.

It has been reported that immersing silk fibroin films in water above 80 °C resulted in the conversion of unordered structures to insoluble β -sheets, although the crystallization temperature of dry silk fibroin resided at about 200 °C.¹⁴ A speculation is that water as a plasticizer provides the silklike blocks conformational flexibility, lowering their crystallization temperature. To examine the role of water in this conformational conversion, SELP-47K nanofibers were baked at 134 °C overnight in a dry oven. No noticeable change in morphology was observed in the baked nanofibers. In marked contrast to the nanofibers that were rendered water insoluble by autoclaving, the baked SELP-47K nanofibers completely dissolved in water.

To analyze the fiber strength, uniaxial stress-strain analysis was conducted on SELP-47K nanofibrous scaffolds, which were autoclaved for 60 min. Five replicate samples of 3 mm in gauge length (between the clamps) were equilibrated in 1 × PBS at 37 °C for 1 h, mounted on a PerkinElmer dynamic mechanical analyzer, and immersed into a jacketed beaker filled with 1 × PBS at 37 °C. Samples were cyclically stretched to 20% strain for 6 cycles, before they were extended to break at around 30% strain (Fig. 3). Displacements were applied at a fixed rate of 0.25 mm/min. The thickness and width of the specimens were measured using optical microscopy⁷ for the calculation of the cross-sectional area and engineering stress. Mechanical analysis of the autoclaved nanofibers yielded a Young's modulus of 1.02 ± 0.28 MPa, an ultimate tensile strength of 0.34 ± 0.04 MPa, and a strain at

failure of $29\% \pm 3\%$. Notably, the autoclaved SELP-47K nanofibrous scaffolds displayed Young's modulus comparable to native elastin.¹⁵ After 6 cycles of mechanical preconditioning, the autoclaved nanofibrous scaffolds exhibited an excellent resilience of $90.7\% \pm 3.4\%$, matching or exceeding native elastin.¹⁵

In summary, autoclaving of SELP-47K nanofibers causes their conversion to water-insoluble, stable materials with excellent mechanical properties suitable, for example, as tissue engineering materials. Our results indicate that autoclaving promotes the formation of ordered β -sheets, functioning as physical crosslinks for the nanofibers. Thus, autoclaving can be used as a chemical-free strategy to physically crosslink recombinant SELP nanofibers.

This work was supported by the NIH (EB009801) and American Heart Association (09BGIA2250621).

¹G. H. Altman, F. Diaz, C. Jakuba, T. Calabro, R. L. Horan, J. S. Chen, H. Lu, J. Richmond, and D. L. Kaplan, *Biomaterials* **24**(3), 401 (2003).

²F. Ferrari and J. Cappello, in *Protein-Based Materials*, edited by K. P. McGrath and D. L. Kaplan (Birkhäuser, Boston, 1997), p. 37.

³J. Cappello, J. W. Crissman, M. Crissman, F. A. Ferrari, G. Textor, O. Wallis, J. R. Whitley, X. Zhou, D. Burman, L. Aukerman, and E. R. Steudensky, *J. Controlled Release* **53**(1-3), **105** (1998).

⁴Z. Megeed, M. Haider, D. Q. Li, B. W. O'Malley, J. Cappello, and H. Ghandehari, *J. Controlled Release* **94**(2-3), 433 (2004).

⁵W. B. Teng, J. Cappello, and X. Y. Wu, *Biomacromolecules* **10**(11), 3028 (2009); W. B. Teng, Y. D. Huang, J. Cappello, and X. Y. Wu, *J. Phys. Chem. B* **115**(7), 1608 (2011).

⁶J. Keyes, M. Junkin, J. Cappello, X. Y. Wu, and P. K. Wong, *Appl. Phys. Lett.* **93**, 023120 (2008).

⁷W. G. Qiu, Y. D. Huang, W. B. Teng, C. M. Cohn, J. Cappello, and X. Y. Wu, *Biomacromolecules* **11**(12), 3219 (2010).

⁸W. G. Qiu, W. B. Teng, J. Y. Cappello, and X. Wu, *Biomacromolecules* **10**(3), 602 (2009).

⁹See supplementary material at <http://dx.doi.org/10.1063/1.3604786> for nanofiber fabrication, FTIR spectra of SELP-47K nanofibers, and band assignment of FTIR spectra.

¹⁰P. Taddei and P. Monti, *Biopolymers* **78**(5), 249 (2005); D. M. Byler and H. Susi, *ibid.* **25**(3), 469 (1986).

¹¹T. Asakura, J. M. Yao, T. Yamane, K. Umemura, and A. S. Ulrich, *J. Am. Chem. Soc.* **124**(30), 8794 (2002).

¹²H. J. Jin and D. L. Kaplan, *Nature* **424**(6952), 1057 (2003).

¹³S. Rammensee, U. Slotta, T. Scheibel, and A. R. Bausch, *Proc. Natl. Acad. Sci. U.S.A.* **105**(18), 6590 (2008).

¹⁴J. Magoshi, M. Mizuide, Y. Magoshi, K. Takahashi, M. Kubo, and S. Nakamura, *J. Polym. Sci., Part B. Polym. Phys.* **17**(3), 515 (1979).

¹⁵C. M. Bellingham, M. A. Lillie, J. M. Gosline, G. M. Wright, B. C. Starcher, A. J. Bailey, K. A. Woodhouse, and F. W. Keeley, *Biopolymers* **70**(4), 445 (2003); J. Gosline, M. Lillie, E. Carrington, P. Guerette, C. Ortlepp, and K. Savage, *Philos. Trans. R. Soc. London, Ser. B* **357**(1418), 121 (2002); B. B. Aaron and J. M. Gosline, *Biopolymers* **20**(6), 1247 (1981).